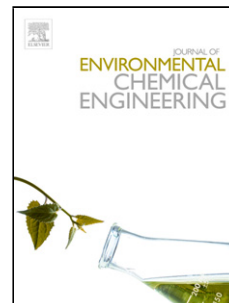# Journal Pre-proof

KINETIC ANALYSIS AND THERMODYNAMICS PROPERTIES OF AIR/STEAM GASIFICATION OF AGRICULTURAL WASTE

Anabel Fernandez (Conceptualization) (Methodology) (Formal analysis) (Investigation) (Writing - original draft) (Software), Leandro Rodriguez Ortiz (Investigation) (Formal analysis), Daniela Asensio (Investigation) (Software), Rosa Rodriguez (Conceptualization) (Resources) (Writing - review and editing) (Supervision) (Project administration) (Funding acquisition), Germán Mazza (Conceptualization) (Resources) (Writing - review and editing) (Supervision) (Project administration) (Funding acquisition)

This is a PDF file of an article that has undergone enhancements after acceptance, such as the addition of a cover page and metadata, and formatting for readability, but it is not yet the definitive version of record. This version will undergo additional copyediting, typesetting and review before it is published in its final form, but we are providing this version to give early visibility of the article. Please note that, during the production process, errors may be discovered which could affect the content, and all legal disclaimers that apply to the journal pertain.

© 2019 Published by Elsevier.

KINETIC ANALYSIS AND THERMODYNAMICS PROPERTIES OF AIR/STEAM GASIFICATION OF AGRICULTURAL WASTE

Anabel Fernandez[a], Leandro Rodriguez Ortiz[a], Daniela Asensio[b],

Rosa Rodriguez[a] and Germán Mazza[b,c],*

[a]Instituto de Ingeniería Química - Facultad de Ingeniería (UNSJ) - Grupo Vinculado al PROBIEN (CONICET-UNCo), San Juan, Argentina

[b]Instituto de Investigación y Desarrollo en Ingeniería de Procesos, Biotecnología y Energías Alternativas, PROBIEN (CONICET-UNCo), Neuquén, Argentina

[c]Centro Científico Tecnológico CONICET - Patagonia Confluencia, Neuquén, Argentina

*(corresponding author) german.mazza@probien.gob.ar (orcid.org/0000-0002-1362-8521)

HIGHLIGHTS

- Macro-TGA applied to gasification of sawdust, plum and olive pits wastes from Cuyo and Northern Patagonia, Argentina
- Model-free approach for kinetic analysis is used.
- A simplified global kinetic model for CO release is developed
- A comparison of previous kinetic analysis using Coats-Redfern method and previous reported data is carried out

Abstract

The air/steam gasification of wood sawdust (SD), plum and olive pits (PP, OP) bio-wastes was studied using macro-thermogravimetric analysis at three heating rates (5, 10, 15 K/min). Three stages were identified during gasification process: water vaporization; de-volatilization and char gasification. The experimental data were analysed by applying five model-free methods: Flynn-Wall-Ozawa (FWO), Distributed Activation Energy Model (DAEM), Friedman, Starink, and Kissinger-Akahira-Sunose (KAS), to evaluate the gasification kinetic parameters. The FWO method exhibited the best fit to the experimental results. The pre-exponential factor was estimated using the Kissinger's expression. The average apparent activation energy (E) for the

char-gasification step was found to be 218.27 (SD), 143.70 (PP) and 87.89 kJ mol^{-1} (OP). The pre-exponential factors were 6.93 10^{23} (SD), 5.10 10^{14} (PP), and 3.71 10^{09} s^{-1} (OP).

A kinetic model to predict the CO release during the bio-waste decomposition was also proposed and validated. The E values for global release of CO were 87.34 (SD), 67.19 (PP), and 133.23 kJ mol^{-1} (OP). In addition, the thermodynamic parameters ΔS, ΔH and ΔG were calculated from the FWO method. The positive values of ΔH evidenced the global endothermicity of the gasification process over the whole range of the conversion degree.

The average ΔG values were 130.53 (SD), 148.17 (PP) and 132.91 kJ mol^{-1} (OP). The average ΔS and ΔG values, together with the Arrhenius kinetic coefficient showed that the reactivity for gasification decreased in the following order: SD > OP > PP. The results are in good agreement with previously reported data.

Keywords: lignocellulosic wastes; gasification; kinetic analysis; model-free methods; macro-TGA.

NOMENCLATURE

A   pre-exponential Arrhenius' factor, 1/s

C   content of carbon, percentage on weight

C_1 constant that depend the reaction stage and the kinetic model, dimensionless

E   activation energy, KJ/mol

ER   equivalence ratio, dimensionless

f(α)   function describing the solid mass changes during the reaction, dimensionless

ΔG   Gibbs free energy change, kJ/mol

h   = 6.63 10^{-34} Js, Plank constant

H   content of hydrogen, percentage on weight

ΔH   enthalpy change, kJ/mol

HHV   higher heating value, MJ/Kg

k   kinetic coefficient, unities depend on the reaction order

k_b = 1.38 10^{-23} J/K, Boltzmann constant

n   reaction order, dimensionless

O   content of oxygen, = C-H-Ash percentage on weight

R   = 8.314 J/(mol K), universal gas constant

ΔS entropy change, kJ/(mol K)

T   temperature, K

T_m temperature of the peak in DTG curves at 5K/min, K

T_{av} reference temperature calculated as the average between the temperature values corresponding to the same degree of conversion obtained at each β condition (Table 3).

t   time, s

V_{CO} yield of gas CO at time t, dimensionless

W_0 initial mass of raw biomass (prior to thermal degradation), g

W_t mass at a generic time, g

W_∞ mass at final condition, after degradation process, g

Greek letters

α degree of conversion, dimensionless

β heating rate, K/min

1. Introduction

Forestry and agro-industrial wastes received minor interest for centuries, but the potential depletion of fossil fuels in the last decades, as well as the need to limit the emissions of greenhouse gases and particulate matters, among other contaminants, have brought renewed interest for their valorization, leading to consider these wastes as valuable raw feedstock for energy and biofuels generation [1,2].

Several technologies have been developed to carry out the thermal conversion of solid biomass into fuels or heat involving pyrolysis, gasification or combustion processes [3,4]. The type of raw

biomass plays a relevant role in the performance of its potential thermal degradation treatment. Agricultural wastes usually tend to have lower lignin contents than woody materials. However, their values fall within the range 15-45 % dry weight, and are adequate to subject these bio-wastes to thermal treatments, like pyrolysis and gasification [5–8]. In addition, the higher the lignin content the higher the H_2 yield in gasification processes is [9]. Another crucial property concerning the biomass composition related to pyrolysis and gasification processes is the ash content. Even if it is usually low in agricultural wastes (12-16 % dry weight), the greater part of the ash will potentially concentrate in the lignin residual fraction, and could hamper the subsequent generation of energy because sintering or fouling effects [10].

When bio-waste is thermally treated, its energy content is released. The biomass is converted into gas, solid (biochar) and liquid (water and *tar*) products. In addition, depending on the process involved, simultaneous or consequent release of thermal energy can occur.

Gasification process allows to convert the carbon and hydrocarbon contents of the bio-wastes into a variety of primaries (syngas -low heating value gas-, biochar, tars, heat) or secondary (electricity, biodiesel, chemicals) products [11]. Additionally, gasification is a very flexible technology. It can be adapted to treat different raw materials, and its operating conditions can be changed selectively to obtain different gaseous products [12]. Air, steam, and oxygen can be used as gasification agent, which severely conditions the resulting syngas composition and heating value, as well as the distribution and by-product yields. Steam gasification produces a syngas with a considerable hydrogen proportion compared to air and oxygen gasification processes [13].

An exhaustive knowledge of the gasification kinetic behaviour for different lignocellulosic bio-wastes is essential to predict experimental yields and to advance in large-scale reactor design.

The macro-TGA technique is a useful tool to gain understanding in the overall chemical reaction kinetics [14]. It is important to note that eventual heat and mass transfer resistances could affect the global decomposition during macro-TGA measurements, as a consequence of the larger particle size and normally higher sample mass used in these experiences (compared to classic

TGA measurements). Consequently, the information from macro-TGA measurements can be used to understand the biomass behavior and tendencies under operating conditions found in industrial devices/processes (commercial scale) and the kinetic parameters obtained will correspond to apparent ones [14]. Nevertheless, relevant observations to heat and mass transfer limitations in such macro-TGA systems were reported by Van de Velden et al. [15] and Brems et al. [16]. These authors concluded that both heat transfer and intra-particle diffusion limitations can be neglected, provided that the experiments are conducted at a low to moderate heating rates and biomass particles size is lower than 300 μm.

Several researchers have used the macro-TGA to study the kinetic behaviour of different biomasses. Skreiberg et al. [17], investigated the pyrolysis behaviour of selected biomass fuels and mixtures (wood, demolition wood, coffee waste and glossy paper) by macro-TGA. Zhou et al. [18] applied macro-TGA to study the pyrolysis hemicellulose, cellulose and lignin (three main biomass components). These researchers concluded that a pyrolysis reaction could be divided into several parallel reactions according to the number of resulting peaks. Sharma and Sheth [19] used this technique to analyse biomass pyrolysis, and they proposed a one-step multi reaction apparent model. Cong et al. [20] evaluated the co-combustion kinetics in macro-TGA of tobacco stalk and low rank coal in blend form. The authors applied Flynn-Wall-Ozawa (FWO) method to predict the activation energy as a function of the reaction conversion over the whole temperature domain. These authors demonstrated that the mixing of tobacco stalk and coal produced an inhibitory interaction before ignition, but it gradually favours the reaction progress when the temperature increases.

Different kinetic methods have been proposed and reported in the literature in order to rationalize the kinetic experimental data. They fit the data obtained using, for instance, macro-TGA and allow to estimate the kinetic parameters that characterize the thermal degradation process [21]. Kinetic models can be classified into model-free, also called isoconversional methods, and model-fitting categories. When applying the isoconversional methods, the kinetic parameters are estimated without adopting an explicit model and the reaction rate is supposed

to be independent to the extent of reaction (conversion) α and depends only on the temperature level (T) [22]. The FWO, Friedman, Starink, KAS and DAEM methods are included in this category.

The main advantages of model-free analysis are the simplicity and the inhibition of errors associated with the selection of a particular kinetic model. On this basis, isoconversional methods can be grouped as [23]:

A) Methods based on the determination of the reaction rate at an equivalent stage for various heating ramps. Friedman method is comprised in this category.

B) Methods based on the temperature integral and requiring data on T_f (β) [24]. DAEM, KAS, FWO and Starink methods [25] are included in this group. These methods comprise a graphic of $1/T_f$ vs. a logarithmic function reliant on heating ramp and it is dependent on the temperature integral used. Each method varies according to the approximation adopted to calculate this integral.

On the other hand, the biomass gasification consists of three stages: drying (evaporation of moisture contained in the solid), de-volatilization (thermal decomposition in the absence of oxygen) and the last step, called char gasification [26]. Meng et al. [27], studied the CO_2 gasification of characteristic components of bio-wastes and the kinetic parameters were obtained using DAEM method. Although the biomass gasification process has been widely studied, only a few works were focused on studying its kinetic behavior. Moreover, research efforts focused on a comparative analysis of the application of isoconversional methods to this process have not been found in the literature, motivating this work. In this context, the objective of this study is to analyse the kinetics of different bio-wastes gasification (sawdust, plum and olive pits) under steam/air atmosphere when heating at three different rates (5, 10, 15 K/min), by using different isoconversional methods.

2. Materials and methods

2.1. Materials

Wood sawdust, plum and olive pits bio-wastes issued from forestry and agro-industries located in Cuyo and Northern Patagonia regions, Argentina, were used in this study. The proximate analysis (moisture, ash and organic matter content) was carried out according to ASTM standards (ASTM E872 - 82; ASTM D1102–84) [28,29] and the elemental analysis was conducted using elemental analyser (AuroEA3000). Lignin, cellulose and hemicellulose contents, were evaluated prior to subject the biomasses to thermal treatments. The lignin, cellulose and hemicellulose contents of the bio-wastes were determined following the American Society for Testing and Materials standards (ASTM D1106-56, ASTM D1103-60 and ASTM D1103-60). The higher heating value (HHV) of the bio-wastes was calculated by using the correlation of Sheng y Azevedo [30] (eq. (1))

HHV [MJ/Kg] = -1.3675 + 0.3137 **C** + 0.7009 **H** + 0.0318 **O** (1)

where **C**, **H** and **O** correspond to the weight percent (wt%) of carbon, hydrogen, and oxygen, respectively, expressed on dry biomass basis.

The validity of this correlation for the bio-wastes studied in this work was discussed by the authors in a previous paper [26].

2.2. Methods

The macro-TGA experiments were carried out in a tubular reactor described in detail by Fernandez et al. [26]. Samples of about 5 g of bio-waste were placed in the crucible. They were previously ground and sieved: only the narrow 212–250 μm fraction was collected for the experiments (in order to avoid heat and mass transfer limitations, according to Van de Velden et al. [15] and Brems et al. [16]). Gasification experiences were conducted under air/steam atmosphere. Steam was generated by pumping water into an evaporator device. The steam flow operating rate was 233 mL/min, with an air flow rate of 26.7 mL/min, at standard conditions.

As discussed by Fernandez et al [26], a low equivalent ratio (ER=0.15) was used because the additional combustion of a fraction of the bio-waste (conventional simultaneous process to provide the heat requirement to the endothermal gasification process in autothermal reactors) is not necessary in the macro-TGA reactor [9,27]. The operating temperature was raised from 300 K to 1173 K at heating rates of 5, 10 and 15 K/min. The experiments were carried out in triplicate. As the standard deviations were smaller than 5%, the average values were used. The CO released in the reactor effluent during the experiments was monitored using a combustion gas analyser TESTO 320, TUV-tested according to EN 50379, Parts 1–3 (EN 50379, 2007).

3. Gasification kinetic analysis

The rate of bio-waste degradation or conversion rate can be expressed in terms of a temperature-dependent specific rate coefficient, k, and a function of the degree of conversion, which is not a temperature-dependent term, $f(\alpha)$. It is expressed in eq. (2):

$$\frac{d\alpha}{dt} = k(T)\, f(\alpha) \tag{2}$$

where α is the degree of conversion of the bio-waste and $f(\alpha)$ is an appropriate function that describes the biomass changes during the chemical reaction. The specific rate coefficient, k, can be expressed by means of the Arrhenius expression (eq. (3))

$$k = A\, e^{-E/RT} \tag{3}$$

E is the activation energy and A the pre-exponential Arrhenius factor also called frequency factor. Additionally, the degree of conversion α can be obtained from each weight loss curve, as stated in eq. (4):

$$\alpha = \frac{W_0 - W_t}{W_0 - W_\infty} \tag{4}$$

where W_0, W_t and W_∞ are the initial mass of the sample, the mass at a given time t, and the mass

of the sample at the final condition of the experiment (after degradation process), respectively.

In order to describe the progress of the reaction in the whole temperature range and for all

temperature-time ramps, the function f(α), and the values of A and E parameters need to be

established. In a general case, the conversion-dependent function f(α) is unknown at the outset

of the study. A range of standard functions representing particular idealised reaction models can

be found in the literature [23].

Table 1 shows the main reactions produced during the gasification [31].

Table 1. Representative chemical reactions during gasification [31].

Heterogeneous reactions	*Homogeneous reactions*
Carbon shift	*Combustion III*
$C + H_2O \leftrightarrow CO + H_2$	$CO + ½ O_2 \leftrightarrow CO_2$
Boudouard reaction	*Water-gas shift reaction*
$C + CO_2 \leftrightarrow 2CO$	$CO_2 + H_2 \leftrightarrow H_2O + CO$
Combustion I	*Steam methane reforming*
$C + ½ O_2 \leftrightarrow CO$	$CH_4 + H_2O \leftrightarrow 3 H_2 + CO$
Combustion II	*Combustion IV*
$C + O_2 \leftrightarrow CO_2$	$½O_2 + H_2 \leftrightarrow H_2O$
Methanation reaction	*Acetone cracking*
$C + 2 H_2 \leftrightarrow CH_4$	$C_6H_6O_6 \leftrightarrow ½C_6H_6O + 1.5 H_2O$
	Phenol cracking
	$C_6H_6O \leftrightarrow ½C_{10}H_8 + CO + H_2$
	Toluene cracking
	$C_7H_8 + H_2 \leftrightarrow C_6H_6 + CH_4$

3.1.   Model-free methods

In this section, a brief description of the isoconversional methods used in the comparative analysis is presented.

3.1.1. Friedman method

Friedman method is a differential isoconversional technique that uses instantaneous rate values [32]. This method constitutes a direct mathematical procedure to estimate the effective activation energy (E), by applying the isoconversional principle to the eq. (2) and replacing k(T) from eq. (3). It is based on particular values of the extent of reaction (or degree of conversion, α), established along the whole macro-TGA experiences regardless of heating ramp. It is founded on the following expression (Friedman equation) [33,34]:

$$k\, f(\alpha) = \ln\, \left(\beta \frac{d\alpha}{dT} \right) = \ln\, [A\, f(\alpha)] - \frac{E}{RT} \tag{5}$$

where $f(\alpha)$, for first order cases, is given by [35]:

$$f(\alpha) = (1-\alpha)^{-n} \tag{6}$$

3.1.2. Distributed activation energy model method (DAEM)

The distributed activation energy model (DAEM), originally developed by Vand [36], has been widely used to study the kinetic behaviour of the complex reactions occurred during the fossil fuels pyrolysis. However, Tran et al. [37] studied the non-isothermal CO_2 gasification of forestry residues and applied DAEM model with four or five pseudo-components. This model is conceived on the basis of the assumption that several parallel irreversible first order reactions with different kinetic parameters are produced simultaneously. As it is reported by Bhavanam

et al. [38], the parameters E and A, can be estimated by the following equation, considering that they are both functions of the temperature:

$$\ln \frac{\beta}{T^2} = \ln \frac{RA}{E} + 0.6075 - \frac{E}{RT} \qquad (7)$$

Eq. (7) shows a linear relationship between $\ln\beta/T^2$ and $1/T$ with the slope equal to $(-E/R)$. The E and A values can be determined from the slope and intercept of the plots.

3.1.3. Kissinger-Akahira-Sunose method (KAS)

This method allows calculating the kinetic parameters of a solid-state reaction without knowing the reaction mechanism and the kinetic parameters can be approximate without the specification of a reaction model. The KAS method is based on the following formulation:

$$\ln \frac{\beta}{T^2} = \ln \frac{AR}{E \, g(\alpha)} - \frac{E}{RT} \qquad (8)$$

where $g(\alpha)$, for a *n-order* reaction is given by:

$$g(\alpha) = n^{-1} \, (-1 + (1-\alpha)^{-n}) \qquad (9)$$

Considering a fixed (constant) value of α, a plot of $\ln(\beta/T^2)$ vs. $1/T$, from the data obtained from the experiences at different heating ramps, leads to develop a straight line. The value of the activation energy E can be obtained from the slope (E/R) of this line.

3.1.4. Flynn-Wall-Ozawa method (FWO)

This method [39, 40] was formulated for non-isothermal analysis. It applies the Doyle's approximation [41] to determine the effective activation energy without specifying the reaction order. Finally, the representative equation of this method can be written as follows:

$$\ln\beta = \ln\frac{EA}{R\,g(\alpha)} - 5.331 - 1.052\,\frac{E}{RT} \tag{10}$$

By plotting ln β vs. 1/T (for a fixed value of α), the value of E can be estimated from experiences conducted at different levels of heating rumps.

3.1.5. Starink method

Starink model-free method allows to calculate the kinetic parameters of a solid-state reaction for different values of the degree of conversion, α. The main equation of this theoretical model can be expressed as [25]:

$$\ln\left(\frac{\beta}{T^{1.8}}\right) = -\frac{AE}{RT} + C_1 \tag{11}$$

where

$$A = 1.0070 - 1.2\,10^{-5}\,E, \text{ (with E values expressed in kJ/mol)} \tag{12}$$

By plotting ln $(\beta/T^{1.8})$ as a function of 1/T, the values of E and A can be easily determined.

3.2.   Simplified kinetic model of CO release

The kinetic model of CO released from gasification process can be described by the eq. (13). The heating ramp as well as the temperature value are required for the application of the model.

$$\frac{d(V_{CO})}{dt} = A\,\exp\left(\frac{E}{RT}\right)(1\text{-}V_{CO})^n \tag{13}$$

where V_{CO} is the yield of CO at a given time t. In eq. (13), A is the pre-exponential factor and n, the reaction order for the global CO release.

According to Ghodke and Mandapati [42], the value of n is equal to 2. The experimental data were fitted to the model expressed in eq. (13) by Nonlinear Least Squares Regression according to the Levenberg-Marquardt algorithm [43,44] in the frame of MATLAB R20155a software.

4. Thermodynamic parameters and pre-exponential factor

The model-free (isoconversional) methods provide accurate values of the activation energy and the values of this kinetic parameter can be used to evaluate the thermodynamic parameters, enthalpy, entropy and Gibbs free energy [45]. Nevertheless, these methods do not allow to predict reliable values of the pre-exponential factor of solid state reactions. Even more, Mishra and Mohanty [46], and Damartzis et al. [47]assert that orders of reaction and pre-exponential factor predicted by the isoconversional methods have no physical meaning. They are merely considered as fitting parameters. In this context, aiming to obtain the values of the thermodynamic parameters (ΔG, ΔH and ΔS) the pre-exponential factor (in terms of the value of the activation energy), was first estimated by the Kissinger's equation (eq. 14) as proposed by Dhyani et al. [45], Yuan et al. [48], Mishra et al. [49], and Xu and Chen [50]:

$$A = \frac{\beta\, E\, \exp\left(\frac{E}{R\, T_m}\right)}{R\, T_m^2} \tag{14}$$

Then, the thermodynamic parameters were evaluated from equations (15-17) [49]:

$$\Delta H = E - RT_m \tag{15}$$

$$\Delta G = E + RT_m\, \ln\left(\frac{k_b T_m}{hA}\right) \tag{16}$$

$$\Delta S = \frac{\Delta H - \Delta G}{T_m} \tag{17}$$

In equations 14-17, T_m is the peak decomposition temperature in the DTG curves [45].

The thermodynamic parameters were calculated for each value of the activation energy obtained by applying the isoconversional method best fitting the experimental data, from the set of five methods described in Section 3. It is important to consider that the interaction between the components increases with the heating rate [51]. In order to minimize such an interaction, the lower heating rate (5 K/min) was selected for T_m.

5. Results and discussion

5.1. Bio-waste characterization

Ultimate and proximate analyses of the studied bio-wastes are shown in Table 2. Considering the first analysis, the olive pits presented the highest bio-wastes carbon (52.79 %) and hydrogen (2.57 %) contents. It is important to remark that these bio-wastes showed a low sulphur content (0.27 - 0.50 %). This condition minimized the SO_x emissions.

Considering the immediate analysis results for the three bio-wastes studied in this work, SD waste presented the greatest moisture content. The ash content can be a hard issue to deal with when using lignocellulosic biomass for energetic purposes due to the presence of alkali metals and chlorine. It may cause the ash components to melt at low temperatures [3]. The three bio-wastes considered in this study (Table 2) had an ash content lower than that of coal (Liu et al. [52] reported the ash content equal to 6.43 and 25.43 wt % for Zhundong coal and Shenhua coal, respectively). Moreover, these low percentages of ash in the studied bio-wastes (Table 2) affect positively the higher heating value (HHV) [53]. The high content of volatile matter made these bio-wastes very suitable to be subjected to thermal treatments [54]. With respect to the lignin contents, the values presented in Table 2 for the three bio-wastes studied fell well within the usual range corresponding to agricultural wastes [8,10,46]. In addition, the fractions of cellulose and hemicellulose (Table 2) are in good agreement with those reported by González-García [8] and Yahya et al. [55]. The composition of the three bio-wastes studied in this work allows to consider them as appropriate to thermal treatments.

Table 2. Results of proximate and ultimate analysis (dry basis, weight percentage). Higher heating values (HHV). From Fernandez et al. [26]

	PP	OP	SD
C (%)	48.95	52.79	44.71
H (%)	1.38	2.57	1.48
N (%)	0.99	1.39	4.20
S (%)	0.27	0.50	0.28
O (%)*	48.41	42.75	49.33
Ash (%, dry basis)	0.73	2.33	1.19
Volatile Matter (%, total weight)	77.86	77.25	80.90
Fixed carbon (%, dry basis)	15.55	15.87	11.06
Moisture (%, total weight)	5.86	4.55	6.85
Lignin (%, dry basis)	42.15	34.27	26.80
Cellulose (%, dry basis)	24.46	31.69	42.96
Hemicellulose (%, dry basis)	21.34	18.41	19.99
HHV (MJ/Kg)	13.71	17.02	12.19

5.2. Weight loss from macro-TGA analysis

Figures 1 and 2 show the weight loss evolution with temperature and their derivative curves (w_t and dw_t/dt, respectively). It can be observed in these curves that the gasification process was carried out following three steps (named step I, II and III, respectively). The first step involves sample heating and weight loss due to the water vaporization (T < 473 K). It represents about 1.82-2.96 % weight loss for the three bio-wastes. The second stage, called de-volatilization, occurs between 473 and 648 K. During this step, the volatile compounds are released and primary char is formed. This is a transition stage with the maximum weight loss and fast decomposition reaction. The weight loss for the three wastes during this step is about 58.96-59.30 %.

The last step, called gasification, occurs between 648 and 1173 K (α range: 0.7 - 0.9), its weight loss represents a 15.82-19.28 % and is mainly associated with the water-gas chemical reaction

to produce CO and H_2. These different ranges are typical for the degradation of lignocellulosic

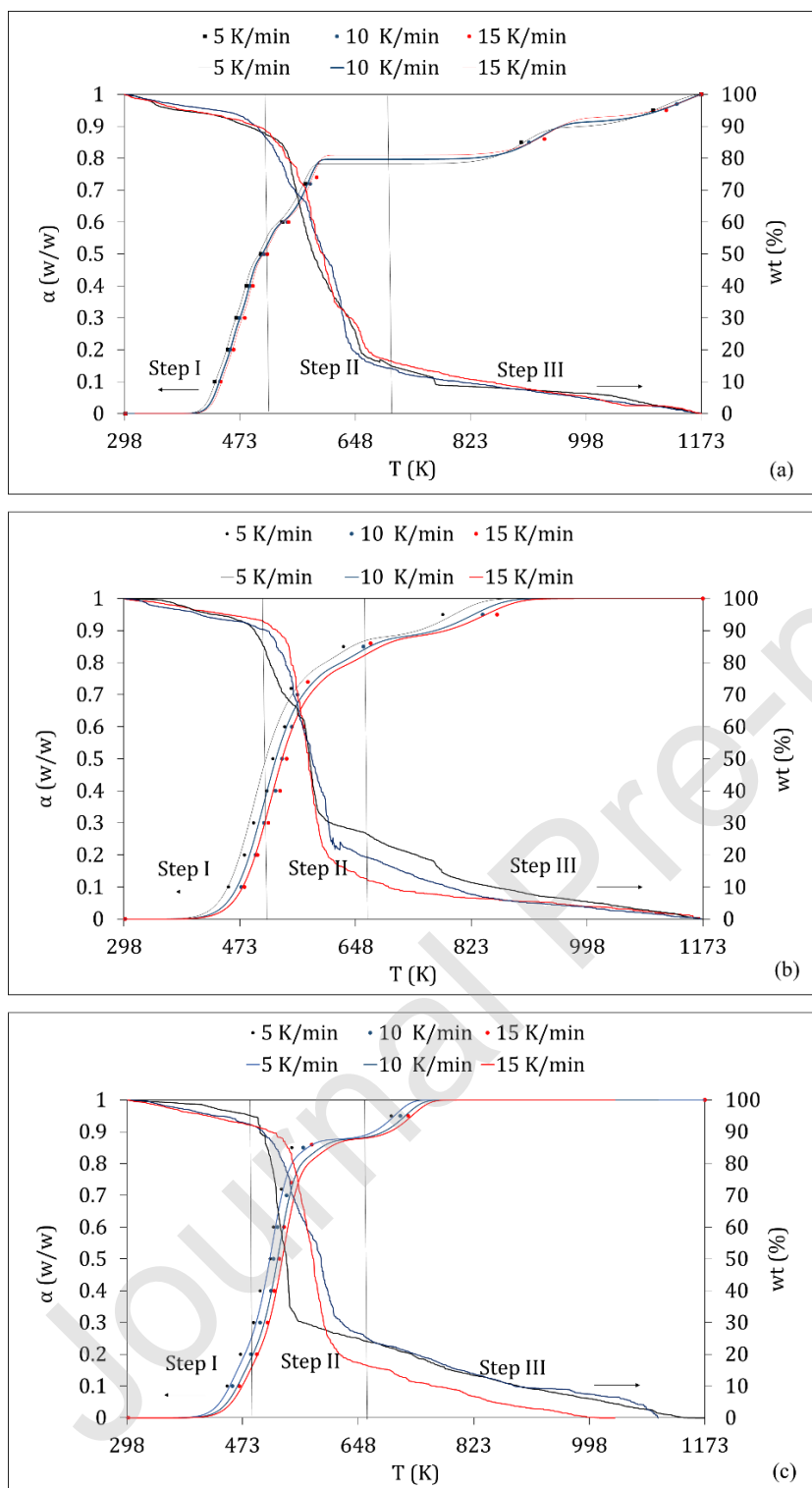biomass, considering that the cellulose, hemicellulose and lignin are the main components [56].

Figure 1. Weight loss (TG curves, w_t vs T) and conversion (α) variation with temperature for

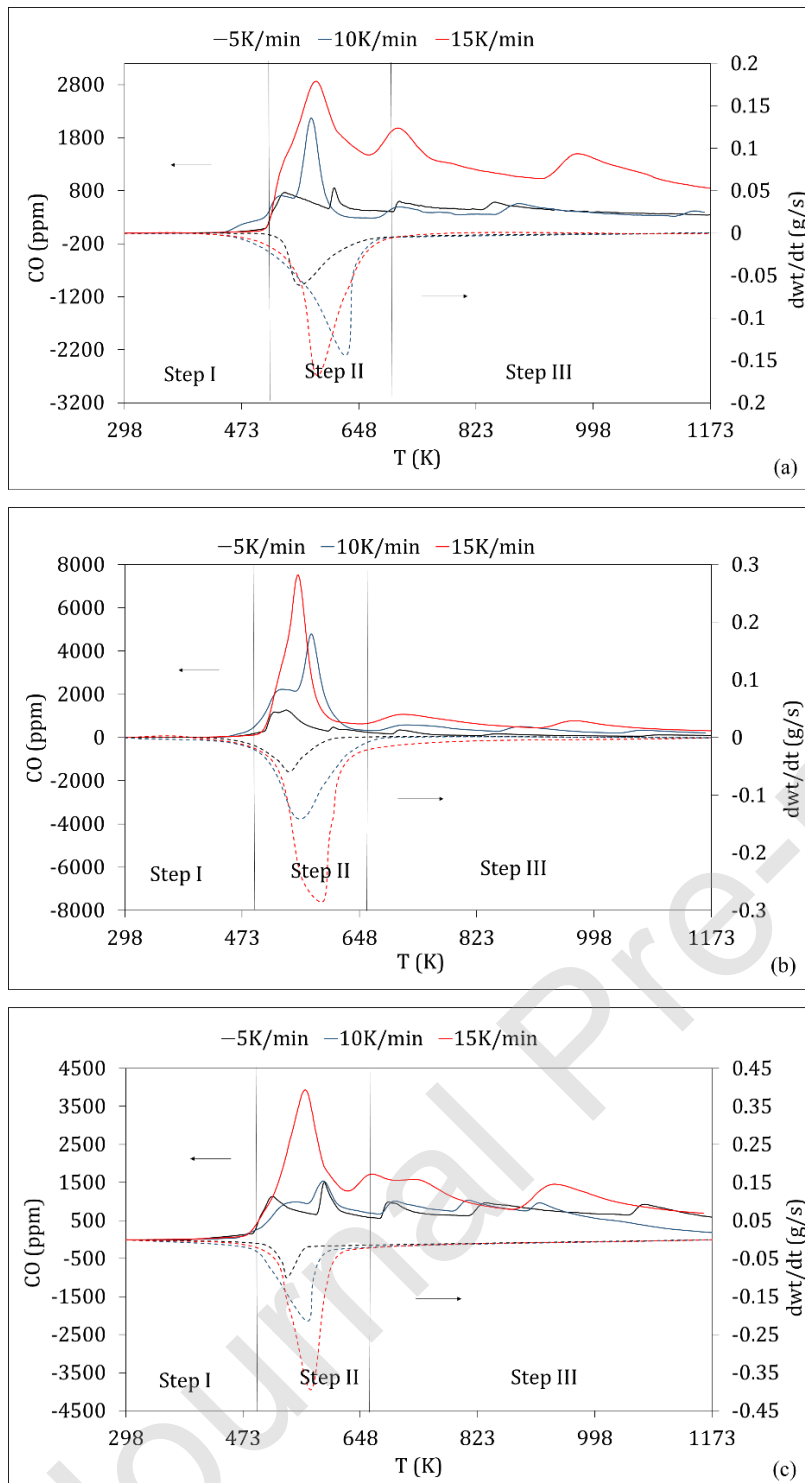(a) SD, (b) PP and (c) OP, at different heating rates.

Figure 2. CO concentration and derivatives curves (DTG curves, dw_t/dt vs T) for (a) SD, (b) PP and (c) OP, at different heating rates.

The derivatives curves show peaks, which are associated to the maximum weight loss rate. This phenomenon occurs at different temperature ranges for the three bio-wasted studied, as follows:

- SD bio-waste, at 524-662 K, 530-670 K and 535-679 K, (α range: 0.4 - 0.6) at heating rates equal to 5, 10 and 15 K/min, respectively.

- OP bio-waste, at 446-606 K, 483-615 K and 502-619 K, (α range: 0.4 - 0.6) at heating rates equal to 5, 10 and 15 K/min, respectively.

- PP bio-waste, at 503-568 K, 524-619 K and 534-627 K (α range: 0.4 - 0.6) at heating rates equal to 5, 10 and 15 K/min, respectively.

The differences between these ranges can be a consequence that biomass degradation depends on its composition, considering that the maximum degradation rate of hemicellulose is carried out between 519 and 568 K, cellulose, between 513 and 612 K, and lignin, between 612 and 653 K [56–58].

5.3. Kinetic analysis

The individual straight-line slope obtained from each isoconversional method (Figure 3) allowed to calculate the activation energy values corresponding to a selected level of α (0.1 to 0.9). It is important to remark here that these values of E were obtained from the isoconversional methods without identifying any reaction model (associated to a reaction mechanism). According to Starink [23], models of the type B (DAEM, KAS, FWO and Starink models) are more accurate than those of type A (like Friedman model). However, in this study, we found similar trends for the activation energy issued from all the methods applied. The small differences observed can be explained based on the calculations techniques and principles of the five methods applied. All the methods except the Friedman one, involve assumptions and particular approximations in the procedure to solve the model's formulation, as it is quoted by Yuan et al. [48].

Table 3 lists the average E values estimated for different values of α, for the three bio-waste samples. The quality of the linear fitting was assessed through the corresponding R^2 values. The extent of each stage of the global gasification process is indicated in Table 3, in terms of the degree of conversion, α. In Table 3, T_{av} is a reference temperature calculated as the average

between the temperature values corresponding to the same degree of conversion obtained at

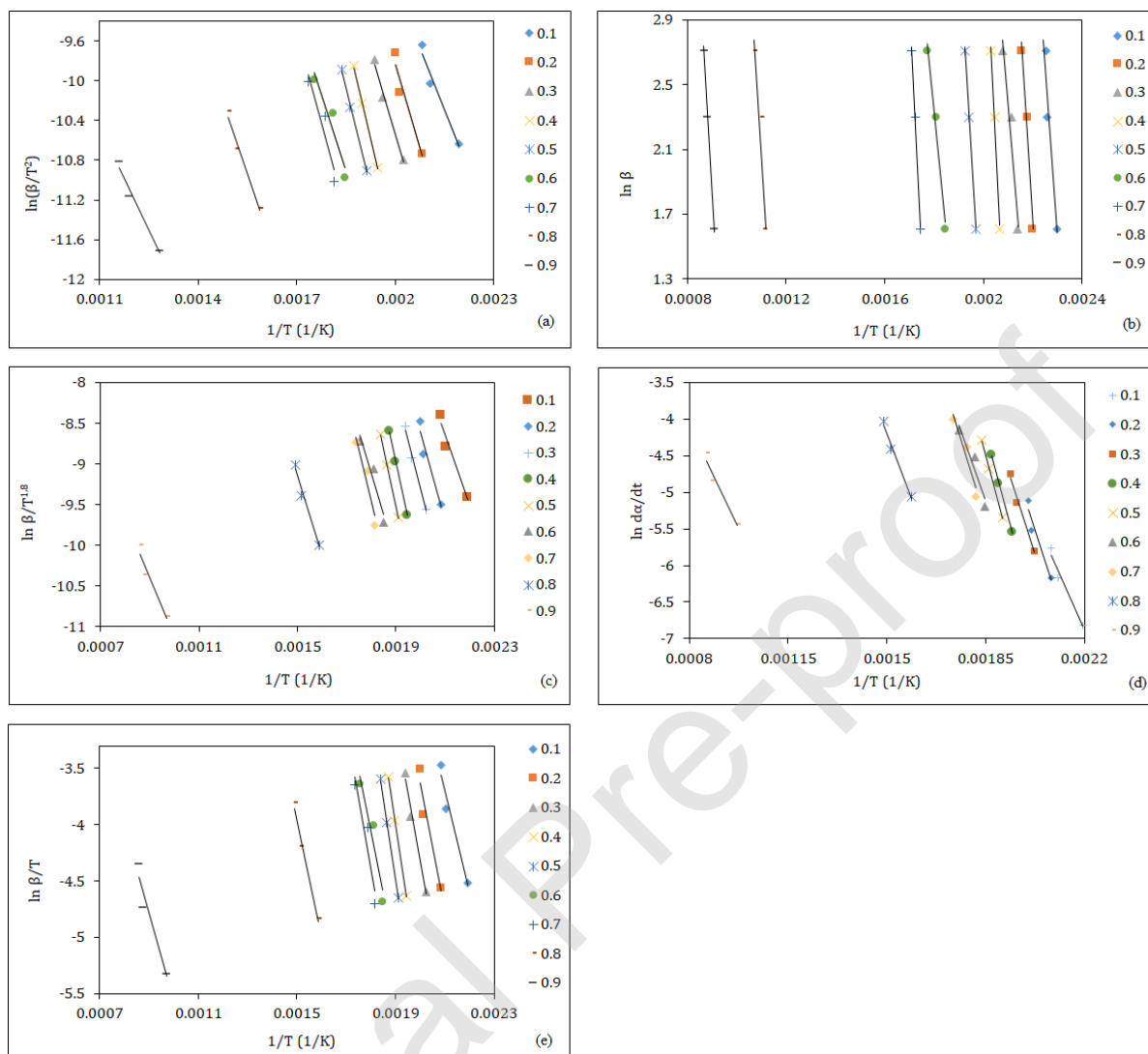each heating rate (β) condition, during a step in the degradation process of a bio-waste.

Figure 3. Linear regression results (conversion α ranging between 10 and 90%) based on (a)

DAEM, (b) FWO, (c) Starink, (d) Friedman and (e) KAS methods, for OP.

Table 3. Activation energy for conversion range 0.1 – 0.9 according to different methods

Bio-wastes	Decomposition stage	α	T_{av} (K)	FWO E (kJ/mol)	R^2	Starink E (kJ/mol)	R^2	Friedman E (kJ/mol)	R^2	DAEM E (kJ/mol)	R^2	KAS E (kJ/mol)	R^2
SD	Dehydration	0.1	440.66	165.35	0.93	166.20	0.92	169.10	0.92	166.65	0.92	166.65	0.92
		0.2	459.33	201.19	0.95	203.32	0.95	206.36	0.95	204.00	0.95	204.00	0.95
		0.3	474.00	149.94	0.92	144.61	0.91	147.75	0.92	144.85	0.91	144.85	0.99
	De-volatilization	0.4	488.66	231.50	0.99	234.56	0.99	237.79	0.99	235.42	0.99	235.42	0.91
		0.5	514.33	192.08	0.99	193.00	0.99	196.39	0.99	193.52	0.99	193.52	0.99
		0.6	553.00	120.84	0.98	118.02	0.97	121.66	0.97	117.93	0.97	117.93	0.98
	Char gasification	0.7	579.33	243.75	0.99	246.01	0.99	249.83	0.99	246.79	0.99	246.79	0.99
		0.8	915.66	197.54	0.90	192.70	0.89	198.76	0.89	192.54	0.89	192.54	0.88
		0.9	1128.66	213.53	0.98	206.37	0.99	213.78	0.98	205.96	0.98	205.96	0.98
	Average			190.64	0.96	189.42	0.96	193.49	0.96	189.74	0.95	189.74	0.95
PP	Dehydration	0.1	458.66	100.49	0.97	93.96	0.95	96.87	0.95	98.08	0.95	98.08	0.96
		0.2	483.66	80.47	0.95	73.61	0.99	76.66	0.99	81.63	0.99	81.63	0.99
		0.3	500.33	103.26	0.99	96.15	0.96	99.31	0.97	100.31	0.96	100.31	0.97
	De-volatilization	0.4	512.33	102.83	0.97	95.58	0.97	98.80	0.97	99.69	0.89	99.69	0.97
		0.5	521.33	160.92	0.91	153.49	0.90	156.80	0.90	160.61	0.97	160.61	0.90
		0.6	527.33	145.44	0.92	137.93	0.91	141.27	0.91	144.23	0.91	144.23	0.91
	Char gasification	0.7	539.66	169.27	0.98	161.59	0.98	165.01	0.99	169.27	0.98	169.27	0.98
		0.8	563.66	92.17	0.99	84.17	0.99	87.73	0.99	87.60	0.99	87.60	0.99
		0.9	711.33	169.65	0.91	159.55	0.98	164.04	0.99	166.66	0.98	166.66	0.99
	Average			124.94	0.95	117.34	0.96	120.72	0.96	123.12	0.96	123.12	0.96
OP	Dehydration	0.1	470.33	74.40	0.97	70.78	0.96	74.39	0.96	70.50	0.95	70.50	0.96
		0.2	492.33	94.72	0.94	91.67	0.93	95.58	0.93	91.51	0.93	91.51	0.93
		0.3	506.66	97.51	0.98	94.37	0.98	98.39	0.98	94.20	0.98	94.20	0.98
	De-volatilization	0.4	525.00	118.49	0.99	115.99	0.99	120.29	0.99	115.11	0.99	115.11	0.99
		0.5	534.66	116.47	0.99	113.74	0.99	118.09	0.99	113.65	0.99	113.65	0.99
		0.6	554.33	89.19	0.92	84.90	0.91	89.21	0.91	84.58	0.91	84.58	0.91
	Char gasification	0.7	562.33	105.36	0.91	101.69	0.89	106.16	0.90	101.47	0.89	101.47	0.90
		0.8	653.66	86.47	0.98	80.69	0.98	85.58	0.90	80.20	0.98	80.20	0.98
		0.9	110.66	71.83	0.94	58.84	0.91	66.51	0.93	57.44	0.97	57.44	0.93
	Average			94.94	0.96	90.30	0.95	94.91	0.94	89.85	0.95	89.85	0.95

The E values during the de-volatilization and char gasification stages varies in the ranges: 99.81 – 179.14 kJ/mol and 79.70 - 215.10 kJ/mol, respectively. The obtained values of E and A can be explained in terms of the collision theory [59] assuming that, for a reaction occurrence, the molecules must collide with one another. But the collisions do not necessarily produce a chemical modification. A collision will be effective only if the molecules possess together a certain threshold of internal energy, equal to E, being the minimum value of energy to react during the gasification process, and depends on the collision frequency (A) between molecules. On this basis, Gai et al. [60] and also Radojević et al. [61] defined the E value as a potential measure of reactivity. According to this criterion, a higher value of this parameter suggests a lower reactivity signifying that a higher amount of energy is required for the reactions to take place.

In this work, E shows a strong dependence on α for all lignocellulosic wastes, indicating the existence of various functional groups with different thermal stability in the biomass [60] and that the gasification process is not a single reaction, characterized by constant E but this process is carried out through complex reaction schemes, including parallel and consecutive reactions [62].

It is observed for the three bio-wastes studied in this work (Table 3) that the variation trend of E with α, is quite similar, regardless of the kinetic methods. This trend depends on the main components (cellulose, hemicellulose and lignin) behaviors due to the fact that the feebler bonds are broken at comparatively lower temperatures than the stronger ones [63].

According to Sittisun et al. [64], the mass loss produced at values of α ≤ 0.15 is linked with the water vaporization. It is important to note that the energy for water vaporization (at small values of α ≤ 0.15) varies, according to the raw biomass. This E variation is explained considering that during drying, the aliphatic hydrogen region is the most active site regarding to reaction with absorbed oxygen [65]. The higher values of E were found for a variable range of α between 0.40 and 0.70, for the three bio-wastes studied, producing an increment of the reaction rate within this range. However, E exhibits a minimum value, corresponding to α values of 0.60 (SD), 0.80

(PP) and 0.90 (OP), respectively. These results explain the observed diminution of the reaction rate at these conversion levels.

According to the definition of Gai et al. [60], a preliminary analysis of the bio-wastes reactivity was performed based on the average values of E. The following order of gasification reactivity was obtained (from the fastest to the slowest global reaction): 89.85 – 94.94 kJ/mol (OP), 117.34 – 124.94 kJ/mol (PP) and 189.74 – 190.64 kJ/mol (SD). The different gasification reactivity can be a consequence of the lignin, cellulose and hemicellulose contents in the bio-wastes. Moreover, secondary reactions may play an important role during the thermal process, influencing the kinetic mechanism (and consequently the E values) [61].

Bearing in mind the E values reported in the literature for the decomposition of pure cellulose (C), hemicelluloses (HC) and lignin (L) during the pyrolysis process (C: 183.81 kJ/mol, HC: 108.65 kJ/mol, and L: 226.24 kJ/mol) [66], the estimated average E values for all bio-wastes were lower than those for the individual pseudo-components. These results can be explained because the decomposition of the bio-wastes was carried out under steam-air atmosphere. During decomposition, the behavior of each pseudo-component determines the generation of different reactive complexes, affecting the global activation energy values and their dependence on the conversion level [67].

With the aim to identify the isoconversional method (from the set of five methods considered in the present study) providing the best fit for the experimental data, a linear regression was carried out based on the main formulation of each method (equations 5 (Friedman), 7 (DAEM), 8 (KAS), 10 (FWO) and 11 (Starink)). For each value of the degree of conversion α in the range 0.1-0.9, a straight line with the corresponding correlation coefficient R^2 was obtained by using data at three different temperatures. It allowed to calculate the value of the activation energy (associated with the fixed value of α). For each method, an average correlation coefficient (for the whole interval of α) was adopted as the decision parameter (acceptance criterion).

This methodology allowed to identify the isoconversional method giving the best fit. On this basis, it was observed that the most accurate values of α as a function of the temperature were

obtained from the FWO model predictions (the average correlation coefficient R^2 is higher than 0.90 for all the analysis, as it is shown in Figure 1).

5.4. **Comparison with previous kinetic analysis using Coats-Redfern method** and other reported data

In a previous work [26], E and A values were determined for both de-volatilization and char gasification stages of SD, PP and OP bio-wastes, using the Coast-Redfern method [68]. For the first step, a first order reaction model showed an adequate fitting and, for the second one, the Ginstling-Brounstein 3D-diffusion model exhibited the best fit. Considering that E and A values, determined by means of this method, are influenced by the heating ramp, the average values of the activation energy ($E_{average}$) and pre-exponential factor ($A_{average}$), are presented in Table 4, identified as **CR*** method. This table also includes the values of $E_{average}$ corresponding to each isoconversional method tested in this study. These average values result from averaging the values of E for the whole interval of the degree of conversion and the three heating ramps studied. The values of the pre-exponential factor $A_{average}$ for the isoconversional methods, was evaluated from Kissinger's expression (eq. 14) as a function of the resulting $E_{average}$ obtained from each isoconversional method. Table 4 includes the results of the average activation energy and pre-exponential factor for both de-volatilization and char-gasification stages.

E varies irregularly with increasing values of heating rate. As a consequence, this parameter does not influence significantly its resulting value. Ma et al. [69] concluded that this dependence is uncertain and E value can be influenced by the biomass composition, size and shape of particle. On the other hand, and bearing in mind the E definition, the reaction with lower activation energy requires a lower temperature or a short reaction time [59].

The values of the pre-exponential factor from Coats-Redfern model-fitting are lower than 10^9 1/s for both stages which would suggest that a closed complex exists (first stage) or a surface reaction is produced (second stage) [70,71].

Table 4. Comparison of de-volatilization/gasification kinetic parameters from isoconversional methods (this work) to Coats-Redfern results [26]

Stage	de-volatilization						char gasification					
Bio-waste	SD		PP		OP		SD		PP		OP	
Methods	$E_{average}$ (kJ/mol)	$A_{average}$ (1/s)	$E_{average}$ (kJ/mol)	$A_{average}$ (1/s)	$E_{average}$ (kJ/mol)	$A_{average}$ (1/s)	$E_{average}$ (kJ/mol)	$A_{average}$ (1/s)	$E_{average}$ (kJ/mol)	$A_{average}$ (1/s)	$E_{average}$ (kJ/mol)	$A_{average}$ (1/s)
FWO (This work)	181.47	3.83×10^{22}	136.40	4.20×10^{13}	108.05	1.42×10^{11}	218.27	6.93×10^{23}	143.70	5.10×10^{14}	87.89	3.71×10^{09}
Starink (This work)	181.86	7.89×10^{22}	129.00	8.47×10^{12}	104.88	7.63×10^{10}	215.03	1.83×10^{24}	135.10	7.71×10^{13}	80.40	1.52×10^{09}
Friedman (This work)	185.28	1.69×10^{23}	132.29	1.73×10^{13}	109.20	2.17×10^{11}	220.79	2.91×10^{24}	138.9	1.77×10^{14}	86.08	4.49×10^{09}
DAEM (This work)	182.29	2.67×10^{22}	134.84	3.91×10^{13}	104.45	6.64×10^{10}	215.10	1.42×10^{24}	134.84	3.84×10^{14}	79.70	1.44×10^{09}
KAS (This work)	182.29	2.67×10^{22}	134.84	3.91×10^{13}	104.45	6.64×10^{10}	215.10	1.42×10^{24}	134.84	3.84×10^{14}	79.70	1.44×10^{09}
CR* ([26])	69.33	8.07×10^{05}	72.33	7.03×10^{06}	80.67	1.03×10^{07}	65.33	3.63×10^{01}	46.67	1.01×10^{0}	39.67	1.67×10^{0}
Modified **CR**** (This work)		4.90×10^{23}		5.61×10^{18}		1.76×10^{15}		3.46×10^{24}		4.91×10^{15}		6.78×10^{11}

* Coats-Redfern method composed of first order reaction model (first step) and Ginstling-Brounstein 3D-diffusion model (second step) [26]
** Pre-exponential factors calculated from Coats-Redfern formulation by introducing E values obtained from FWO method

The Coats-Redfern activation energy values obtained from this approach (CR*) [26], are significantly lower than the values calculated from the five isoconversional methods studied in this work. It can be seen that the activation energy values calculated from Coats-Redfern approach (with both reaction order n=1and n ≠1) for the pyrolysis of pine sawdust biomass (PSB) and sal sawdust biomass (SSB) reported by Mishra and Mohanty [49] are quite similar to the gasification values issued from Coats-Redfern method [68]. These researchers reported E=50.19 KJ/mol (PSB, n ≠1), 64.13 (PSB, n=1), 43.89 (SSB, n≠1), and 57.97 (n=1). To the authors' knowledge, no prior studies in addition to that published by Fernandez et al. [26] have reported results based on the Coats-Redfern method for biomass gasification in order to evaluate the activation energy. However, Daneshvar et al. [72] reported the same tendency with respect to Coats-Redfern activation energy values with respect to FWO, Friedman and KAS results, for the pyrolysis of a green macro algae, Codium Fragile (C. Fragile).

Based on the reactivity definition of Gai et al. [60], and applying the Coast-Redfern method during the de-volatilization stage (with the highest mass loss), the SD bio-waste showed the highest reactivity (E average equal to 69.27 kJ/mol) [26]. However, when using the isoconversional methods, OP bio-waste presented the highest reactivity. This observation can be due to the different hypothesis and assumptions adopted in the models' formulations [46]. It is necessary to consider that the evaluation of the activation energy from Coats-Redfern approach was considered as a risky alternative [73]. On the contrary, the isoconversional methods are simple in their basis, and most remarkable advantage is that there is no risk to select a wrong kinetic model and to find wrong kinetic parameters [73]. On this basis, the observation regarding the reactivity based on isoconversional methods could be considered as more reliable.

No significant differences were found between pre-exponential factors calculated from the Kissinger's equation for the different bio-wastes, using the values of E obtained from the five isoconversional methods studied in this work. However, the E value issued from the FWO method is considered as the most appropriate, based on the criteria explained in Section 5.3.

Finally, it is important to note here that the model-free methods can consistently estimate E and A (this last parameter, evaluated by means of an additional expression like Kissinger's equation (eq. 14)), but the obtained data are limited because these methods do not allow to determine the corresponding kinetic mechanism (and reaction order) [46,49]. The values of the activation energy obtained from an isoconversional method can be used to check the pre-exponential factor and the complete kinetic model [45]. Consequently, the activation energy from the FWO method can be introduced into the formulation of the Coats-Redfern model-fitting method to estimate the pre-exponential factor. The corresponding average pre-exponential factor values issued from these procedure (called Modified Coats-Redfern method in this contribution) are also included in Table 4. As it can be observed, these values follow the tendency of the pre-exponential factor corresponding to the isoconversional methods (eq. 14).

The values of the pre-exponential factor from the modified Coats-Redfern approach are closer to the Kissinger's expression than those obtained by the original Coat-Redfern approach. This is consistent with the statements quoted by Mishra and Mohanty [46] and Mishra et al. [49] with respect to the risk of using the Coats-Redfern method to evaluate the activation energy.

Due to the bio-waste heterogeneity, it is crucial to analyze the reaction mechanism using model-fitting methods. In this context, it can be concluded that both methods should be considered as complementary. Thus, the identification of the complete reaction mechanism and the evaluation of the average pre-exponential factor can be carried out by means of the methodology proposed in this work.

A comparison of the average E values obtained from isoconversional methods with previous results reported in the literature is summarized in Table 5. Considering the diverse biomass sources and characteristics, and the different gasification agents, it can be seen that the average activation energy values obtained in this study from the FWO method are, in general, in good agreement with previously reported data for similar biomasses (experimental and modelling results obtained by different techniques and models). Only PP bio-waste exhibits a relatively low value of the activation energy. It can be due to a complex structure of the solid matrix.

Table 5. Comparison of gasification activation energy values with data reported in the literature.

Bio-waste	β (K/min)	Gasification agent	$E_{average}$ (kJ/mol)	References
Palm shells, coconut shells and bamboo guadua	10	steam	134	Romero Millan et al. (2019) [74]
(TC+bio-waste blends)* 1)TC/CM 2)TC/EFB 3)TC/AS 4)TC/RSS	15-60	CO_2	1) 185.54 2) 230.79 3) 233.73 4) 209.60	Lahijani et al. (2019) [75]
Beech wood char	24	steam	167	Dupont et al. (2011) [76]
Wood char (RDC)	n/d	steam	204	Paviet et al. (2007) [77]
Different biomasses	n/d	steam	40-240	Di Blasi (2009) [3]
Beech wood chips (char)	n/d	1) steam 2) CO_2	1) 139 2) 154	Guizani et al. (2013) [78]
Microalgae Chlorella vulgaris	10-40	Argon/steam	187-198	Figueira et al. (2015) [79]
Wood Sawdust	5-15	steam	218.27	This work
Plum Pit	5-15	steam	143.70	This work
Olive Pit	5-15	steam	87.89	This work

* *(CM): cattle manure, (EFB): palm empty fruit bunch, (AS): almond shell; (RSS): rubber seed shell; (TC): tire char.*

5.5. Simplified kinetic model for CO release

This gaseous compound released during the de-volatilization and gasification steps. Figure 2 shows that the higher the heating rate, the higher the observed CO released. During the de-volatilization stage, the maximum CO concentration was obtained (473 - 648 K) [26]. For the SD bio-waste, more than 40, 46 and 52% of CO released before 580, 582 and 591 K for 5, 10 and 15 K/min, respectively. In the case of OP bio-waste, the produced CO volume fraction was 49, 51 and 58% before 546, 570 and 561 K, for 5, 10 and 15 K/min, respectively. Finally, the PP bio-waste presented values of 38, 42 and 59% of CO released before 580, 605 and 571 K, for 5, 10 and 15 K/min, respectively. At temperatures higher than 648 K, tar formed during the first stage may thermally decompose and generate CO, among other products, detecting reduced peaks of CO release [26].

Considering the main components hemicellulose, cellulose and lignin, it is important to note that a considerable amount of CH_4 is produced, when the lignin content in the biomass is high. However, if the hemicellulose and cellulose contents are high, the CO release is significant [80]. This aspect would justify the observed variation of CO amount released during the experiences, taking into account the different decomposed bio-wastes. A high concentration of CO in the gaseous product can be generated due to cracking of carbonyl and carboxyl groups (from hemicellulose and cellulose decomposition) and secondary reactions of primary volatiles (from lignin decomposition) [80].

The proposed kinetic model for predicting the CO release during the bio-wastes decomposition, presented a good fit to the experimental data (Figure 4). The R^2 coefficient values were higher than 0.9 in all cases (Table 6). The resulting values of the kinetic parameters E and A are listed in Table 6 for all bio-wastes studied and for the different heating rate conditions tested. When the heating ramp increased, an augmentation of the activation energy and a decrease in the biomass reactivity were observed.
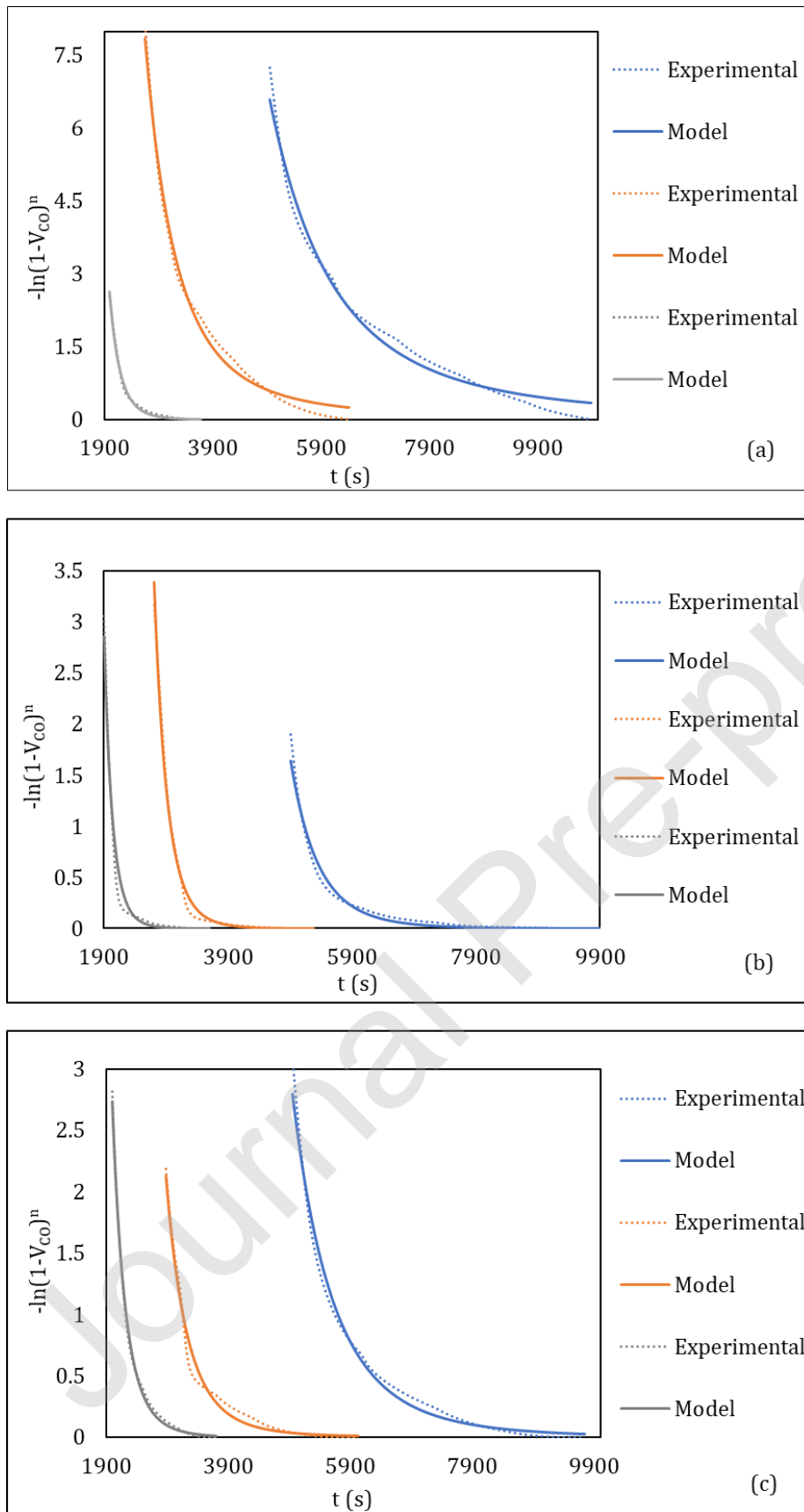
Figure 4. CO release evolution. Comparison of experimental and predicted values by kinetic modeling CO evolution for (a) PP, (b) SD and (c) OP, at different heating rates.

The lowest value of E was 42.63 kJ/mol for PP bio-waste at 5 K/min and the highest, 150.70 kJ/mol for OP bio-waste at 15 K/min. This activation energy is a global value related to all chemical reactions realising CO.

Table 6. Pre-exponential factor and activation energy obtained by kinetic modeling of CO evolution.

Bio-wastes	β (K/min)	E (KJ/mol)	A (s^{-1})	R^2
SD	5	75.52	7.91×10^{-6}	0.99
	10	87.03	3.02×10^{-6}	0.98
	15	99.47	8.11×10^{-7}	0.99
PP	5	42.63	4.87×10^{-3}	0.98
	10	46.83	3.88×10^{-3}	0.99
	15	112.10	1.21×10^{-7}	0.99
OP	5	113.3	7.10×10^{-9}	0.98
	10	135.70	1.20×10^{-9}	0.99
	15	150.70	1.07×10^{-10}	0.98

5.6. Thermodynamic analysis

In addition to the kinetic parameters, the estimation of thermodynamic parameters allows to define the feasibility of the thermal decomposition process and to evaluate the energy requirements.

Figure 5 shows the resulting values of ΔG, ΔH and ΔS for the three biomass samples studied in this work. It is important to remark that these thermodynamic properties were calculated by

using the activation energy values obtained from the FWO method. The FWO method was selected because it presented the best fit for the degree of conversion, as explained in Section 5.3. In spite of this situation, no significant differences were obtained by using the other isoconversional methods studied in this work.
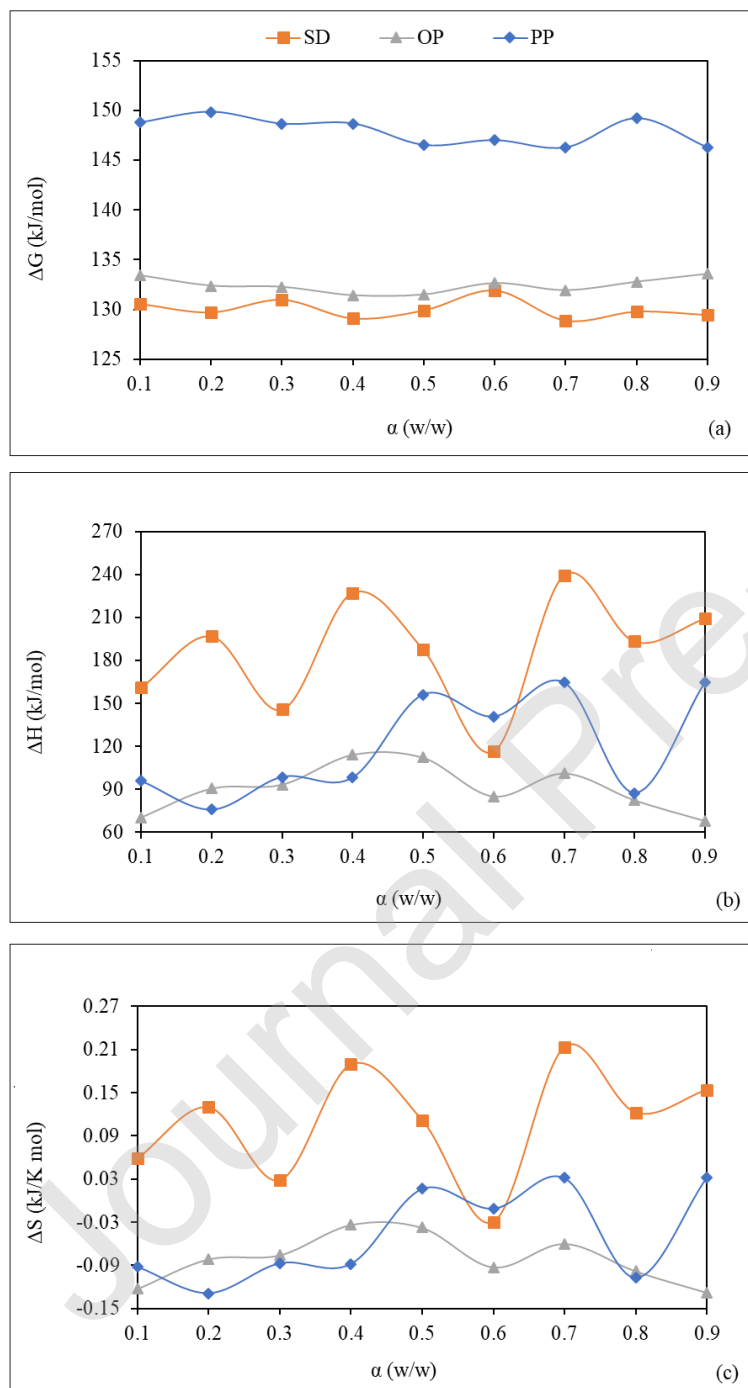

Figure 5. Thermodynamic parameters as a function of α, evaluated from the FWO method for SD, OP and PP bio-wastes.

The change of entropy (ΔS) is a measure of the disorder degree in a system. A small value of ΔS defines a low reactivity of the system analysed, indicating that the bio-waste has been transformed by some chemical process, transporting it to a state close to its own thermodynamic equilibrium [81]. On the other hand, a negative value of ΔS means that the disorder degree of products formed by bond rupture was inferior to that of the initial reactants.

 All bio-wastes studied in this work presented both, negative and positive values, considering the entire temperature and degree of conversion ranges of analysis. The values of ΔS fell in the ranges -0.04 to 0.22, -0.14 to 0.03 and -0.16 to -0.03 kJ/(mol K), for SD, PP and OP, respectively. As calculated ΔS values were small in some cases, it can be asserted that the bio-wastes had a low reactivity, being more difficult to form the activated complex. Higher values of ΔS indicate the higher reactive characteristic of the bio-waste (the SD samples, in this work).

The difference in enthalpy ΔH is a relevant thermodynamic parameter that represents the total heat content of the system, particularly the thermal energy between the state of reactant species and that of the activated complex [50]. ΔH defines the thermal characteristic of the chemical reaction (exothermic or endothermic). The ΔH values were comprised between 113.62 – 245.53, 68.83 – 164.49 and 53.15 – 116.01 kJ/mol, for SD, PP and OP, respectively. These values clearly indicate that an external energy source is required to reach the transition state. Therefore, the gasification process is endothermic in the whole range of α. Small ΔH values favours the formation of activated complex. In this context, this formation is observed at α values equal to 0.6 for SD, 0.8 for PP; and 0.9 for OP [50]. The greater ΔH values were found for the SD bio-waste (Figure 5b), due to the fact that its gasification requires a higher amount of energy than the other bio-wastes to dissociate the bonds of reactants. The ΔH values obtained for the three bio-wastes were similar to those corresponding to the pyrolysis of isolated pseudo-components, hemicellulose: 150.96 kJ/mol, cellulose: 168.23 kJ/mol and lignin: 239.74 kJ/mol reported by Yuan et al. [48].

Finally, ΔG is the change of the Gibbs free energy, representing the total energy increase of the chemical reaction system for the formation of the activated complex. It is a widespread analysis

of the heat flow and disorder change. The spontaneity of the activated complex formation is determined according to the sign and magnitude of ΔG (a negative sign of ΔG indicates a spontaneous formation of the activated complex from reagents, while the higher the positive ΔG value the lower the spontaneity of the reaction is [82]). The resulting ΔG values were in the ranges 129.08 – 131.98, 146.27 – 150.06 and 131.41 – 134.41 kJ/mol, for SD, PP and OP bio-wastes, respectively, for values of the degree of conversion α within the range 0.1-0.9. As it can be observed, these values of ΔG are positives in all cases, revealing the total energy rise of the system at the approach of the reagents and the formation of the activated complex, as quoted by Xu and Chen [50]. The change in Gibbs free energy indicates that during the formation of the activated complex the total energy of the reaction system increases. The highest average value of ΔG was obtained for PP bio-waste (147.90 kJ/mol) and the lowest for SD bio-waste (130 kJ/mol), being consistent with the reactivity tendency based on ΔS values. Therefore, PP bio-waste showed the lowest reaction spontaneity. A light increase is observed for the ΔG in the studied range of the degree of conversion. In addition, the average values of ΔG are lower than the corresponding average values of ΔG reported by Yuan et al [48] for the pyrolysis of hemicellulose, cellulose, and lignin components (165.39, 164.87, and 163.37 kJ/mol, respectively). The tendency for the gasification of the three studied bio-waste is then, to be more spontaneous than the individual pyrolysis of the three mentioned main biopolymers.

Dhyani et al., [45] stated that the value of the pre-exponential factor is a measure of reactivity. In the present work, the combined effect of both, the average activation energy and the pre-exponential factor is tested by means of the kinetic coefficient from the Arrhenius' expression (eq. 3), as an indicator of the potential of reactivity. For instance, considering the char-gasification step at a conversion degree of α=0.8 (mean value of the α range for the gasification step), the kinetic coefficient for the three bio-wastes studied was estimated at T_{av} values of 915.66 K (SD), 563.66 K (PP) and 653.66 K (OP). By using the $E_{average}$ values from FWO method (Table 4) and the $A_{average}$ values calculated by Kissinger's expression (eq. 14), the following values of the kinetic coefficient k, arose: 2.37 1011 1/s (SD bio-waste), 3,49 102 1/s (OP bio-

waste) and 2.42 101 1/s (PP bio-waste). From the magnitude of the kinetic coefficient evaluated at the same degree of conversion for the gasification step it can be inferred that the potential reactivity of the three bio-wastes studied for gasification decomposition in descending order is : SD > OP > PP and is consistent with the conclusion obtained on the basis of the thermodynamic parameters ΔG and ΔS.

The SD is the bio-waste showing the most spontaneous characteristic regarding gasification.

The values of ΔG and ΔH obtained for SD, OP and PP bio-wastes in this work were in good agreement with the data reported by Lahijani et al. [75] for CO_2 co-gasification of several bio-wastes, including cattle manure (CM), palm empty fruit bunch, almond shell (AS) and rubber seed shell (RSS) with tire char (TC). The gasification of different blends of these biomasses with TC was investigated at different heating rates by non-isothermal thermogravimetric method.

6. CONCLUSIONS

In this work, a macro-TGA kinetic study of the gasification of wood sawdust, plum pit and olive pit bio-wastes, under an atmosphere of air and steam was carried. The treatment of the experimental data was performed applying different isoconversional methods: Flynn-Wall-Ozawa (FWO), Distributed Activation Energy Model (DAEM), Friedman, Starink, and Kissinger-Akahira-Sunose (KAS). The FWO method provided the best fitting of the experimental results and is proposed as the method to evaluate the activation energy. Compared to the results of activation energy from Coats-Redfern for gasification of the same bio-wastes previously published, these values were quite different. In this frame, the behavior of the model-free methods and Coats-Redfern method was critically analyzed.

Taking into account the potential information that could be obtained from FWO (including the pre-exponential factor from Kissinger's expression as a function of E) and Coats-Redfern methods (to identify the reaction mechanism and to determine the reaction order), a complementary combined methodology was used and proved to be suitable for the kinetic characterization of the gasification process of lignocellulosic biomasses.

With respect to reactivity characteristics, the tendency obtained from the main thermodynamic parameters ΔS and ΔG (evaluated using the apparent activation energy values obtained by FWO method) together with the values of the specific kinetic coefficient (Arrhenius low), allowed to establish that the reactivity of the three bio-wasted studied for gasification decomposition decreased in the following order: SD > OP > PP. The spontaneity, given by the ΔG sign and magnitude, positioned the three bio-wastes having low spontaneity for the gasification process. Nevertheless, a slight advantage is displayed in favor of sawdust bio-waste.

The proposed model for the release of CO during the different stages of the global process revealed that the CO emission was higher during de-volatilization stage, but its evolution continues along the char gasification stage. In addition, for three wastes the kinetic parameters of CO evolution were obtained. The activation energy suggested that lower emission should be expected from PP bio-wastes.

The results obtained in the different topics of the present work are in reasonable agreement with previously reported data.

CRediT authorship contribution statement
Anabel Fernandez: Conceptualization, Methodology, Formal analysis, Investigation, Writing - original draft; Software
Leandro Alexei Rodriguez Ortiz: Investigation, Formal analysis,
Daniela Asensio: Investigation, Software.
Rosa Rodriguez: Conceptualization, Resources, Writing - review & editing, Supervision, Project administration, Funding acquisition.
Germán Mazza: Conceptualization, Resources, Writing - review & editing, Supervision, Project

administration, Funding acquisition.

Declaration of interests

The authors declare that they have no known competing financial interests or personal relationships that could have appeared to influence the work reported in this paper.

REFERENCES

[1]   H.B. Goyal, D. Seal, R.C. Saxena, Bio-fuels from thermochemical conversion of renewable resources: A review, Renew. Sustain. Energy Rev. 12 (2008) 504–517. https://doi.org/10.1016/J.RSER.2006.07.014.

[2]   P. Sette, A. Fernandez, J. Soria, R. Rodriguez, D. Salvatori, G. Mazza, Integral valorization of fruit waste from wine and cider industries, J. Clean. Prod. 242 (2020) 118486. https://doi.org/10.1016/J.JCLEPRO.2019.118486.

[3]   C. Di Blasi, Combustion and gasification rates of lignocellulosic chars, Prog. Energy Combust. Sci. 35 (2009) 121–140. https://doi.org/10.1016/J.PECS.2008.08.001.

[4]   J. Soria, K. Zeng, D. Asensio, D. Gauthier, G. Flamant, G. Mazza, Comprehensive CFD modelling of solar fast pyrolysis of beech wood pellets, Fuel Process. Technol. 158 (2017) 226–237. https://doi.org/10.1016/J.FUPROC.2017.01.006.

[5]   S. Adhikari, H. Nam, J.P. Chakraborty, Conversion of Solid Wastes to Fuels and Chemicals Through Pyrolysis, Waste Biorefinery. (2018) 239–263. https://doi.org/10.1016/B978-0-444-63992-9.00008-2.

[6]   P. Kumar, D.M. Barrett, M.J. Delwiche, P. Stroeve, Methods for Pretreatment of Lignocellulosic Biomass for Efficient Hydrolysis and Biofuel Production, Ind. Eng. Chem. Res. 48 (2009) 3713–3729. https://doi.org/10.1021/ie801542g.

[7]   H. Hartmann, Solid Biofuelssolid biofuel, Fuels and Their Characteristics, in: R.A. Meyers

(Ed.), Encycl. Sustain. Sci. Technol., Springer New York, New York, NY, 2012: pp. 9821–9851. https://doi.org/10.1007/978-1-4419-0851-3_245.

[8]   P. González-García, Activated carbon from lignocellulosics precursors: A review of the synthesis methods, characterization techniques and applications, Renew. Sustain. Energy Rev. 82 (2018) 1393–1414. https://doi.org/10.1016/J.RSER.2017.04.117.

[9]   M. Echegaray, D.Z. García, G. Mazza, R. Rodriguez, Air-steam gasification of five regional lignocellulosic wastes: Exergetic evaluation, Sustain. Energy Technol. Assessments. 31 (2019) 115–123. https://doi.org/10.1016/j.seta.2018.12.015.

[10]   Q. Kang, L. Appels, T. Tan, R. Dewil, Bioethanol from Lignocellulosic Biomass: Current Findings Determine Research Priorities, Sci. World J. 2014 (2014) 298153. https://doi.org/10.1155/2014/298153.

[11]   G. Skodras, G. Nenes, N. Zafeiriou, Low rank coal – CO2 gasification: Experimental study, analysis of the kinetic parameters by Weibull distribution and compensation effect, Appl. Therm. Eng. 74 (2015) 111–118. https://doi.org/10.1016/J.APPLTHERMALENG.2013.11.015.

[12]   T.P. Thomsen, Z. Sárossy, B. Gøbel, P. Stoholm, J. Ahrenfeldt, F.J. Frandsen, U.B. Henriksen, Low temperature circulating fluidized bed gasification and co-gasification of municipal sewage sludge. Part 1: Process performance and gas product characterization, Waste Manag. 66 (2017) 123–133. https://doi.org/10.1016/J.WASMAN.2017.04.028.

[13]   A.K. James, S.S. Helle, R.W. Thring, P.M. Rutherford, M.S. Masnadi, Investigation of Air and Air-Steam Gasification of High Carbon Wood Ash in a Fluidized Bed Reactor, Energy Environ. Res. 4 (2014) 15–24. https://doi.org/10.5539/eer.v4n1p15.

[14]   D. Tapasvi, R. Khalil, Ø. Skreiberg, K.Q. Tran, M. Grønli, Torrefaction of Norwegian birch and spruce: An experimental study using macro-TGA, Energy and Fuels. 26 (2012) 5232–5240. https://doi.org/10.1021/ef300993q.

[15]   M. Van de Velden, J. Baeyens, A. Brems, B. Janssens, R. Dewil, Fundamentals, kinetics and endothermicity of the biomass pyrolysis reaction, Renew. Energy. 35 (2010) 232–242.

https://doi.org/10.1016/J.RENENE.2009.04.019.

[16] A. Brems, J. Baeyens, J. Beerlandt, R. Dewil, Thermogravimetric pyrolysis of waste polyethylene-terephthalate and polystyrene: A critical assessment of kinetics modelling, Resour. Conserv. Recycl. 55 (2011) 772–781. https://doi.org/10.1016/J.RESCONREC.2011.03.003.

[17] A. Skreiberg, O. Skreiberg, J. Sandquist, L. Sørum, TGA and macro-TGA characterisation of biomass fuels and fuel mixtures, Fuel. 90 (2011) 2182–2197. https://doi.org/10.1016/j.fuel.2011.02.012.

[18] H. Zhou, Y. Long, A. Meng, S. Chen, Q. Li, Y. Zhang, A novel method for kinetics analysis of pyrolysis of hemicellulose, cellulose and lignin in TGA and macro-TGA, RSC Adv. 5 (2015) 26509–26516. https://doi.org/10.1039/C5RA02715B.

[19] R. Sharma, P.N. Sheth, Multi reaction apparent kinetic scheme for the pyrolysis of large size biomass particles using macro-TGA, Energy. (2018). https://doi.org/10.1016/J.ENERGY.2018.03.075.

[20] K. Cong, F. Han, Y. Zhang, Q. Li, The investigation of co-combustion characteristics of tobacco stalk and low rank coal using a macro-TGA, Fuel. 237 (2019) 126–132. https://doi.org/10.1016/J.FUEL.2018.09.149.

[21] A. Khawam, D.R. Flanagan, Solid-state kinetic models: Basics and mathematical fundamentals, J. Phys. Chem. B. 110 (2006) 17315–17328. https://doi.org/10.1021/jp062746a.

[22] A.K. Burnham, R.L. Braun, Global Kinetic Analysis of Complex Materials, Energy & Fuels. 13 (1999) 1–22. https://doi.org/10.1021/ef9800765.

[23] M.J. Starink, The determination of activation energy from linear heating rate experiments: A comparison of the accuracy of isoconversion methods, Thermochim. Acta. 404 (2003) 163–176. https://doi.org/10.1016/S0040-6031(03)00144-8.

[24] M.J. Starink, Kinetic equations for diffusion-controlled precipitation reactions, J. Mater. Sci. 32 (1997) 4061–4070. https://doi.org/10.1023/A:1018649823542.

[25]   M.J. Starink, Heating rate dependence of precipitation in an Al-1%Si alloy, J. Mater. Sci. Lett. 15 (1996) 1749–1751. https://doi.org/10.1007/BF00275330.

[26]   A. Fernandez, J. Soria, R. Rodriguez, J. Baeyens, G. Mazza, Macro-TGA steam-assisted gasification of lignocellulosic wastes, J. Environ. Manage. 233 (2019) 626–635. https://doi.org/10.1016/j.jenvman.2018.12.087.

[27]   A. Meng, S. Chen, Y. Long, H. Zhou, Y. Zhang, Q. Li, Pyrolysis and gasification of typical components in wastes with macro-TGA, Waste Manag. 46 (2015) 247–256. https://doi.org/10.1016/j.wasman.2015.08.025.

[28]   E872 - 82 ASTM, Standard Test Method for Volatile Matter in the Analysis of Particulate Wood Fuels, ASTM Int. (1998) 14–16. https://doi.org/10.1520/E0872-82R06.2.

[29]   D1102–84 ASTM, Standard Test Method for ash in wood, ASTM Int. (2001) 2. https://doi.org/10.1520/D1894-14.2.

[30]   C. Sheng, J.L.T. Azevedo, Estimating the higher heating value of biomass fuels from basic analysis data, Biomass and Bioenergy. 28 (2005) 499–507. https://doi.org/10.1016/j.biombioe.2004.11.008.

[31]   J. Yu, J.D. Smith, Validation and application of a kinetic model for biomass gasification simulation and optimization in updraft gasifiers, Chem. Eng. Process. - Process Intensif. 125 (2018) 214–226. https://doi.org/10.1016/j.cep.2018.02.003.

[32]   H.L. Friedman, Kinetics of thermal degradation of char-forming plastics from thermogravimetry. Application to a phenolic plastic, J. Polym. Sci. Part C Polym. Symp. 6 (1964) 183–195. https://doi.org/10.1002/polc.5070060121.

[33]   P. Simon, Isoconversional methods: Fundamentals, meaning and application, J. OfThermal Anal. Calorim. 76 (2004) 123–132. https://doi.org/10.1023/B.

[34]   A. Aboulkas, K. El Harfi, Study of the kinetics and mechanisms of thermal decomposition of Moroccan Tarfaya oil shale and its kerogen, Oil Shale. 25 (2008) 426–443. https://doi.org/10.3176/oil.2008.4.04.

[35]   A. Garcia-Maraver, J.A. Perez-Jimenez, F. Serrano-Bernardo, M. Zamorano, Determination

and comparison of combustion kinetics parameters ofagricultural biomass from olive trees, Renew. Energy. 83 (2015) 897–904. https://doi.org/10.1016/j.renene.2015.05.049.

[36] V. Vand, A theory of the irreversible electrical resistance changes of metallic films evaporated in vacuum, Proc. Phys. Soc. 55 (1943) 222. http://stacks.iop.org/0959-5309/55/i=3/a=308.

[37] K.Q. Tran, H.H. Bui, A. Luengnaruemitchai, L. Wang, Ø. Skreiberg, Isothermal and non-isothermal kinetic study on CO2 gasification of torrefied forest residues, Biomass and Bioenergy. 91 (2016) 175–185. https://doi.org/10.1016/j.biombioe.2016.05.024.

[38] A. Bhavanam, R.C. Sastry, Kinetic study of solid waste pyrolysis using distributed activation energy model, Bioresour. Technol. 178 (2015) 126–131. https://doi.org/10.1016/j.biortech.2014.10.028.

[39] J.H. Flynn, L.A. Wall, A quick, direct method for the determination of activation energy from thermogravimetric data, J. Polym. Sci. Part B Polym. Lett. 4 (1966) 323–328. https://doi.org/10.1002/pol.1966.110040504.

[40] T. Ozawa, A New Method of Analyzing Thermogravimetric Data, Bull. Chem. Soc. Jpn. 38 (1965) 1881–1886. https://doi.org/10.1246/bcsj.38.1881.

[41] C.D. Doyle, Estimating isothermal life from thermogravimetric data, J. Appl. Polym. Sci. 6 (1962) 639–642. https://doi.org/10.1002/app.1962.070062406.

[42] P. Ghodke, R.N. Mandapati, Investigation of particle level kinetic modeling for babul wood pyrolysis, Fuel. 236 (2019) 1008–1017. https://doi.org/10.1016/J.FUEL.2018.09.084.

[43] K. Levenberg, A method for the solution of certain non-linear problems in least squares, Q. Appl. Math. 2 (1944) 164–168. http://www.jstor.org/stable/43633451.

[44] D.W. Marquardt, An Algorithm for Least-Squares Estimation of Nonlinear Parameters, J. Soc. Ind. Appl. Math. 11 (1963) 431–441. https://doi.org/10.1137/0111030.

[45] V. Dhyani, J. Kumar, T. Bhaskar, Thermal decomposition kinetics of sorghum straw via thermogravimetric analysis, Bioresour. Technol. 245 (2017) 1122–1129.

https://doi.org/10.1016/J.BIORTECH.2017.08.189.

[46] R.K. Mishra, K. Mohanty, Pyrolysis kinetics and thermal behavior of waste sawdust biomass using thermogravimetric analysis, Bioresour. Technol. 251 (2018) 63–74. https://doi.org/10.1016/J.BIORTECH.2017.12.029.

[47] T. Damartzis, D. Vamvuka, S. Sfakiotakis, A. Zabaniotou, Thermal degradation studies and kinetic modeling of cardoon (Cynara cardunculus) pyrolysis using thermogravimetric analysis (TGA), Bioresour. Technol. 102 (2011) 6230–6238. https://doi.org/10.1016/j.biortech.2011.02.060.

[48] X. Yuan, T. He, H. Cao, Q. Yuan, Cattle manure pyrolysis process: Kinetic and thermodynamic analysis with isoconversional methods, Renew. Energy. 107 (2017) 489–496. https://doi.org/10.1016/j.renene.2017.02.026.

[49] R.K. Mishra, K. Mohanty, X. Wang, Pyrolysis kinetic behavior and Py-GC–MS analysis of waste dahlia flowers into renewable fuel and value-added chemicals, Fuel. 260 (2020) 116338. https://doi.org/10.1016/J.FUEL.2019.116338.

[50] Y. Xu, B. Chen, Investigation of thermodynamic parameters in the pyrolysis conversion of biomass and manure to biochars using thermogravimetric analysis, Bioresour. Technol. 146 (2013) 485–493. https://doi.org/10.1016/J.BIORTECH.2013.07.086.

[51] H. Cao, Y. Xin, D. Wang, Q. Yuan, Pyrolysis characteristics of cattle manures using a discrete distributed activation energy model, Bioresour. Technol. 172 (2014) 219–225. https://doi.org/10.1016/J.BIORTECH.2014.09.049.

[52] Y. Liu, L. Cheng, J. Ji, W. Zhang, Ash deposition behavior in co-combusting high-alkali coal and bituminous coal in a circulating fluidized bed, Appl. Therm. Eng. 149 (2019) 520–527. https://doi.org/10.1016/J.APPLTHERMALENG.2018.12.080.

[53] G. San Miguel, F. Gutiérrez Martín, Technologies for the use and transformation of biomass-to-energy. (in Spanish), Mundi-Prensa, Madrid, Spain, 2015.

[54] A. Demirbas, Effects of temperature and particle size on bio-char yield from pyrolysis of agricultural residues, J. Anal. Appl. Pyrolysis. 72 (2004) 243–248.

https://doi.org/10.1016/j.jaap.2004.07.003.

[55] M.A. Yahya, Z. Al-Qodah, C.W.Z. Ngah, Agricultural bio-waste materials as potential sustainable precursors used for activated carbon production: A review, Renew. Sustain. Energy Rev. 46 (2015) 218–235. https://doi.org/10.1016/J.RSER.2015.02.051.

[56] A.K. Burnham, L.N. Dinh, A comparison of isoconversional and model-fitting approaches to kinetic parameter estimation and application predictions, J. Therm. Anal. Calorim. 89 (2007) 479–490. https://doi.org/10.1007/s10973-006-8486-1.

[57] S.D. Stefanidis, K.G. Kalogiannis, E.F. Iliopoulou, C.M. Michailof, P.A. Pilavachi, A.A. Lappas, Journal of Analytical and Applied Pyrolysis A study of lignocellulosic biomass pyrolysis via the pyrolysis of cellulose , hemicellulose and lignin, 105 (2014) 143–150.

[58] J.F. González, S. Román, J.M. Encinar, G. Martínez, Pyrolysis of various biomass residues and char utilization for the production of activated carbons, J. Anal. Appl. Pyrolysis. 85 (2009) 134–141. https://doi.org/10.1016/J.JAAP.2008.11.035.

[59] J.E. White, W.J. Catallo, B.L. Legendre, Biomass pyrolysis kinetics: A comparative critical review with relevant agricultural residue case studies, J. Anal. Appl. Pyrolysis. 91 (2011) 1–33. https://doi.org/10.1016/j.jaap.2011.01.004.

[60] C. Gai, Y. Dong, T. Zhang, The kinetic analysis of the pyrolysis of agricultural residue under non-isothermal conditions, Bioresour. Technol. 127 (2013) 298–305. https://doi.org/10.1016/J.BIORTECH.2012.09.089.

[61] M. Radojević, B. Janković, V. Jovanović, D. Stojiljković, N. Manić, Comparative pyrolysis kinetics of various biomasses based on model-free and DAEM approaches improved with numerical optimization procedure, PLoS One. 13 (2018) 1–25. https://doi.org/10.1371/journal.pone.0206657.

[62] R. Kaur, P. Gera, M.K. Jha, T. Bhaskar, Pyrolysis kinetics and thermodynamic parameters of castor (Ricinus communis) residue using thermogravimetric analysis, Bioresour. Technol. 250 (2018) 422–428. https://doi.org/10.1016/J.BIORTECH.2017.11.077.

[63] Z. Dong, J. Cai, Isoconversional kinetic analysis of sweet sorghum bagasse pyrolysis by

modified logistic mixture model, J. Energy Inst. (2017). https://doi.org/10.1016/j.joei.2017.04.006.

[64] P. Sittisun, N. Tippayawong, D. Wattanasiriwech, Thermal Degradation Characteristics and Kinetics of Oxy Combustion of Corn Residues, Adv. Mater. Sci. Eng. 2015 (2015) 1–8. https://doi.org/10.1155/2015/304395.

[65] A. Tahmasebi, J. Yu, Y. Han, X. Li, A study of chemical structure changes of Chinese lignite during fluidized-bed drying in nitrogen and air, Fuel Process. Technol. 101 (2012) 85–93. https://doi.org/10.1016/j.fuproc.2012.04.005.

[66] L. Abdelouahed, S. Leveneur, L. Vernieres-Hassimi, L. Balland, B. Taouk, Comparative investigation for the determination of kinetic parameters for biomass pyrolysis by thermogravimetric analysis, J. Therm. Anal. Calorim. 129 (2017) 1201–1213. https://doi.org/10.1007/s10973-017-6212-9.

[67] F.C. Beall, Thermogravimetric analysis of wood lignin and hemicelluloses, Wood Fiber Sience. 3 (1969) 215–226.

[68] A.W. Coats, J.P. Redfern, Kinetic parameters from thermogravimetric data, Nature. 201 (1964) 68–69. http://dx.doi.org/10.1038/201068a0.

[69] Z. Ma, J. Wang, Y. Yang, Y. Zhang, C. Zhao, Y. Yu, S. Wang, Comparison of the thermal degradation behaviors and kinetics of palm oil waste under nitrogen and air atmosphere in TGA-FTIR with a complementary use of model-free and model-fitting approaches, J. Anal. Appl. Pyrolysis. 134 (2018) 12–24. https://doi.org/10.1016/J.JAAP.2018.04.002.

[70] S. Wang, B. Ru, H. Lin, Z. Luo, Degradation mechanism of monosaccharides and xylan under pyrolytic conditions with theoretic modeling on the energy profiles, Bioresour. Technol. 143 (2013) 378–383. https://doi.org/10.1016/J.BIORTECH.2013.06.026.

[71] C. Di Blasi, Modeling chemical and physical processes of wood and biomass pyrolysis, Prog. Energy Combust. Sci. 34 (2008) 47–90. https://doi.org/10.1016/j.pecs.2006.12.001.

[72] S. Daneshvar, F. Salak, K. Otsuka, Pyrolytic Behavior of Green Macro Algae and Evaluation

of Its Activation Energy, Int. J. Chem. Eng. Appl. 3 (2012) 256–263. https://doi.org/10.7763/ijcea.2012.v3.196.

[73]   M. Alwani, A.K. H.P.S, O. Sulaiman, M.N. Islam, R. Dungani, An Approach to Using Agricultural Waste Fibres in Biocomposites Application: Thermogravimetric Analysis and Activation Energy Study, BioResources. 9 (2013). https://doi.org/10.15376/biores.9.1.218-230.

[74]   L.M. Romero Millán, F.E. Sierra Vargas, A. Nzihou, Steam gasification behavior of tropical agrowaste: A new modeling approach based on the inorganic composition, Fuel. 235 (2019) 45–53. https://doi.org/10.1016/J.FUEL.2018.07.053.

[75]   P. Lahijani, M. Mohammadi, A.R. Mohamed, Investigation of synergism and kinetic analysis during CO2 co-gasification of scrap tire char and agro-wastes, Renew. Energy. 142 (2019) 147–157. https://doi.org/10.1016/J.RENENE.2019.04.113.

[76]   C. Dupont, T. Nocquet, J.A. Da Costa, C. Verne-Tournon, Kinetic modelling of steam gasification of various woody biomass chars: Influence of inorganic elements, Bioresour. Technol. 102 (2011) 9743–9748. https://doi.org/10.1016/J.BIORTECH.2011.07.016.

[77]   F. Paviet, B. Olivier, A. Gérard, Kinetic Study of Various Chars Steam Gasification, Int. J. Chem. React. Eng. 5 (2007). https://doi.org/10.2202/1542-6580.1460.

[78]   C. Guizani, F.J. Escudero Sanz, S. Salvador, The gasification reactivity of high-heating-rate chars in single and mixed atmospheres of H2O and CO2, Fuel. 108 (2013) 812–823. https://doi.org/10.1016/J.FUEL.2013.02.027.

[79]   C.E. Figueira, P.F. Moreira, R. Giudici, Thermogravimetric analysis of the gasification of microalgae Chlorella vulgaris, Bioresour. Technol. 198 (2015) 717–724. https://doi.org/10.1016/J.BIORTECH.2015.09.059.

[80]   A. Saffe, A. Fernandez, M. Echegaray, G. Mazza, R. Rodriguez, Pyrolysis kinetics of regional agro-industrial wastes using isoconversional methods, Biofuels. 7269 (2017) 1–13. https://doi.org/10.1080/17597269.2017.1316144.

[81]   L.T. Vlaev, I.G. Markovska, L.A. Lyubchev, Non-isothermal kinetics of pyrolysis of rice

husk, Thermochim. Acta. 406 (2003) 1–7. https://doi.org/10.1016/S0040-6031(03)00222-3.

[82] J. Sheng, D. Ji, F. Yu, L. Cui, Q. Zeng, N. Ai, J. Ji, Influence of Chemical Treatment on Rice Straw Pyrolysis by TG-FTIR, IERI Procedia. 8 (2014) 30–34. https://doi.org/10.1016/J.IERI.2014.09.006.

Figure 1. Weight loss (TG curves, w_t vs T) and conversion (α) variation with temperature for (a) SD, (b) PP and (c) OP, at different heating rates.

Figure 2. CO concentration and derivatives curves (DTG curves, dw_t/dt vs T) for (a) SD, (b) PP and (c) OP, at different heating rates.

Figure 3. Linear regression results (conversion α ranging between 10 and 90%) based on (a) DAEM, (b) FWO, (c) Starink, (d) Friedman and (e) KAS methods, for OP.

Figure 4. CO release evolution. Comparison of experimental and predicted values by kinetic modeling CO evolution for (a) PP, (b) SD and (c) OP, at different heating rates.

Figure 5. Thermodynamic parameters as a function of α, evaluated from the FWO method for SD, OP and PP bio-wastes.
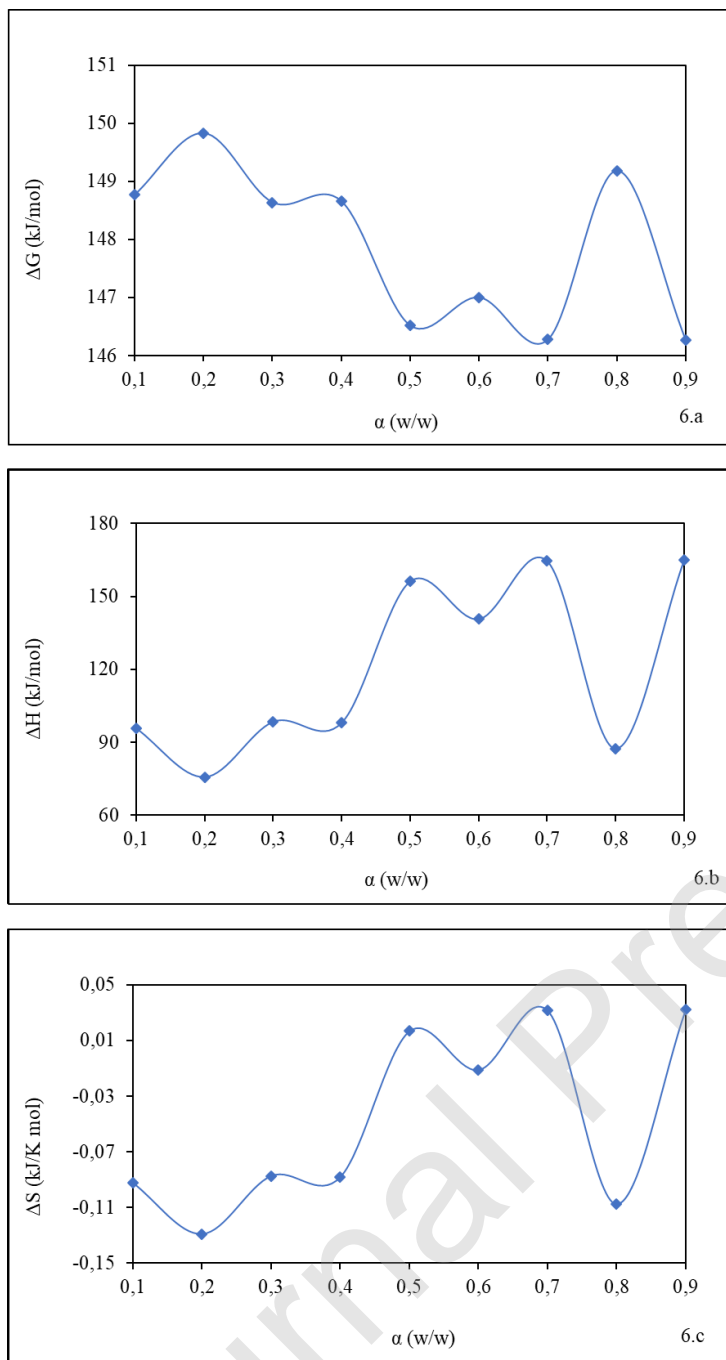
Figure 6

Figure 7

7.a

7.b

7.c